Oxidation of Metals, Vol. 15, Nos. 5/6, 1981

The Growth and Structure of Oxide Films on Fe. I. Oxidation of (001) and (112) Fe at 200–300°C

M. J. Graham* and R. J. Hussey*

Received April 22, 1980—Revised June 16, 1980

A study has been made of the oxidation of (001) and (112) Fe at 200–300°C in 5×10^{-3} Torr O_2 to determine the influence of substrate orientation and surface pretreatment. Using oxidation kinetics, reflection electron diffraction, and electron optical techniques, it has been shown that the nature of the prior oxide film has a marked effect on oxidation behavior for a given orientation. The initial faster rate for a surface covered with a 16-Å prior oxide film formed by dry oxidation at room temperature is attributed to a smaller subgrain size in this film, compared to that for a prior film formed by electropolishing. This initial rapid rate is not sustained because of oxide separation from the metal. α-Fe_2O_3 formation, which occurs at higher temperatures for either surface pretreatment, is enhanced by the oxide separation.

KEY WORDS: iron oxidation; single crystals; surface pretreatment; oxide grain size.

INTRODUCTION

Previous work has shown the oxidation rate of Ni single crystals at 600°C in 5×10^{-3} Torr O_2 to be strongly dependent upon metal orientation and surface pretreatment.[1] Different surface pretreatments produced structurally different prior oxide films. Where a single-orientation prior oxide was produced and maintained during subsequent oxidation, the oxidation rate was very low. If the oxide became twinned, comprising one or two sets of twin-related orientations, the oxidation rate was increased, and if in the extreme case, the oxide became polycrystalline, the oxidation rate was increased by a factor of 10^4. In the present work single crystals of Fe have

*Division of Chemistry, National Research Council of Canada, Ottawa, Canada K1A 0R9.

0030-770X/81/0600-0407$03.00/0

been oxidized to oxide thicknesses of the same order of magnitude as for the Ni single crystals with a view to examining the influences of oxide structure and surface pretreatment on the oxidation rate. Fe (001) and (112) surfaces were selected because these orientations have been examined previously in reflection electron diffraction studies of the nature of oxide films and have shown markedly different oxidation behavior.[2,3] The Fe system is more complex than the Ni case, because of inferior oxide adhesion and the possibility of multiple phase formation, namely, α-Fe_2O_3 in addition to the cubic, spinel-type oxide.[4]

EXPERIMENTAL

Surface Preparation

Fe single-crystal specimens* (0.1 cm thick and ~ 1 cm^2 in surface area) with (001) or (112) surfaces were prepared using an abrasive wire saw. Specimens were chemically polished in a H_2O_2–oxalic acid solution, spark-planed, again chemically polished, mechanically polished through 0.1-μ diamond and then electropolished in perchloric–acetic acid.[5] Specimens were then given a vacuum anneal at 700°C for 2 hr, re-electropolished and installed in a high-vacuum manometric apparatus.

Oxidation Procedure

Specimens were oxidized either in the electropolished condition (EP), or after reduction of the electropolish film in H_2 at 600°C followed by cooling in H_2 and preoxidation at room temperature in 5×10^{-3} Torr O_2 (HR + O). This latter treatment produced an oxide film of similar thickness (~ 16 Å) to that formed after EP and was selected, because it had been determined that Ni surfaces so conditioned oxidized much more rapidly than those given the EP treatment.[1] Oxidation was initiated by a "furnace-raised" procedure in which the specimens were heated in less than 1 min to the oxidation temperature in 5×10^{-3} Torr O_2 using an infrared radiation furnace.[1] Temperatures were measured and controlled by means of a 0.013-cm diam. Pt/Pt–Rh thermocouple spot-welded to the specimen. The O_2 uptake during oxidation was monitored by following the decrease in pressure with time. At the pressure used weight changes of ~ 0.025 μg·cm^{-2} (~ 2 Å oxide) could be detected.

*Minimum 99.96% Fe. Major impurities (ppm by weight): B 16, C 12, O 54, P 11, S 63, Ti 4, Cr 5, Mn 3, Co 41, Ni 160, Cu 19, Ge 4, Mo 9.

Oxide Examination

The prior oxides formed after the two surface pretreatments (EP or HR + O), and those produced on subsequent oxidation at temperatures up to 300°C, were structurally characterized by reflection electron diffraction (RED). Some oxides could be "dry-stripped" from their substrates during two stage replication and these were examined by transmission electron microscopy (TEM).

RESULTS

Oxidation Kinetics

The kinetic data for both the HR + O and EP surfaces oxidized at 240, 260, and 300°C are shown in Figs. 1, 2, and 3, respectively. The degree of reproducibility of the kinetics is indicated in the figures and in Tables I and II. At each temperature the (001) and (112) surfaces oxidize at similar rates for a given surface pretreatment. While the extent of O_2 uptake for the HR + O surfaces was greater over the first few minutes, the later stages were characterized by a decrease to a low rate of oxidation. The final weight gains were less than those for the EP surfaces, the difference becoming larger at higher temperatures. In contrast to the lower temperatures the oxidation rates of EP surfaces at 300°C also decreased to low values at long times (Fig. 3).

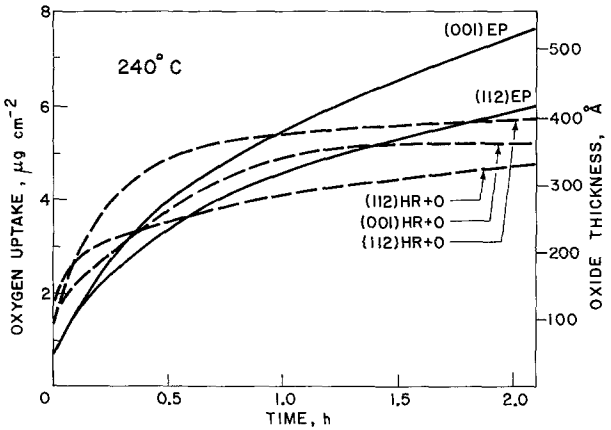

Fig. 1. Oxidation kinetics of (001) and (112) EP Fe (solid curves) compared to those of (001) and (112) HR + O Fe (broken curves) at 240°C.

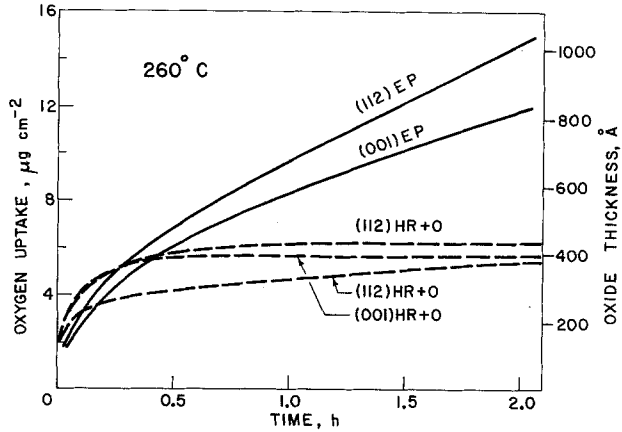

Fig. 2. Oxidation kinetics of (001) and (112) EP Fe (solid curves) compared to those of (001) and (112) HR + O Fe (broken curves) at 260°C.

The oxidation results summarized in Tables I and II show that the oxide films in general could be entirely "dry-stripped" with great ease from the HR + O surfaces. Void formation and separation at the metal–oxide interface is thus indicated and the poorer reproducibility for the HR + O runs is not surprising in view of the random nature of this process.

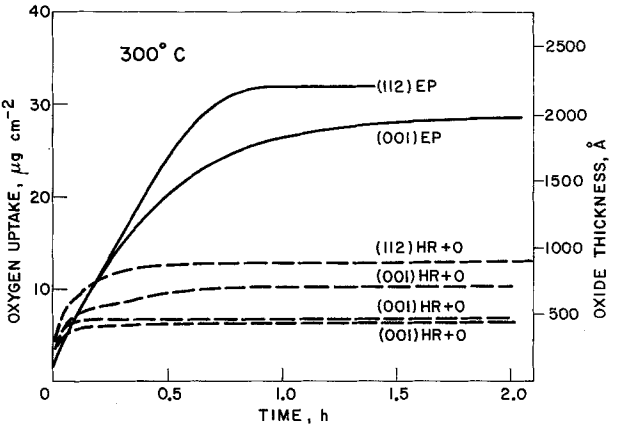

Fig. 3. Oxidation kinetics of (001) and (112) EP Fe (solid curves) compared to those of (001) and (112) HR + O Fe (broken curves) at 300°C.

Table I. Oxidation of (001) Fe—Summary of Results

Preparation	Temp., (°C)	Time, hr	Oxide thickness, Å	Oxides found[a] RED	Oxides found[a] TED	Oxide adherence[b]
EP	200	2.01	144	M	—	—
EP	220	2.08	315	M	—	—
EP	240	2.13	499	M	—	good
EP	240	2.04	526	—	—	good
EP	260	2.04	838	M	M[d]	fair
EP	300	0.12	312	M	—	good
EP	300	2.05	1996	H	M, H	good[c]
HR+O	240	2.05	364	M	M	poor
HR+O	260	2.10	396	—	M, H	poor
HR+O	300	2.00	711	M, H	—	poor
HR+O	300	2.03	439	—	M, H	poor
HR+O	300	2.00	466	H	—	poor

[a] M ≡ Fe_3O_4; H ≡ α-Fe_2O_3; predominant oxide is underlined.
[b] Good ≡ less than 1% removed; fair ≡ less than 50% removed; and poor ≡ greater than 50% removed during replication.
[c] Film removed from substrate by electropolishing.
[d] α-Fe_2O_3 also evident from replica.

Table II. Oxidation of (112) Fe—Summary of Results

Preparation	Temp., °C	Time, hr	Oxide thickness, Å	Oxides found[a] RED	Oxides found[a] TED	Oxide adherence[b]
EP	200	2.13	95	M, H^{ES}	—	good
EP	220	2.08	194	M, H^{ES}	M	fair
EP	240	2.16	340	M, H^{ES}	—	—
EP	240	2.15	420	M, H^{ES}	M	fair
EP	260	2.05	1045	M, H^{ES}	—	good
EP	300	0.17	547	M	—	good
EP	300	1.41	2230	H	—	good
HR+O	240	0.26	265	M, H	—	good
HR+O	240	2.05	401	M, H	M, H	poor
HR+O	240	2.10	331	M, H	M	poor
HR+O	260	2.15	380	M, H^{ES}	M, H	poor
HR+O	260	2.10	431	M, H	—	fair
HR+O	300	2.10	903	H	M, H	poor

[a] M ≡ Fe_3O_4; H ≡ α-Fe_2O_3; predominant oxide is underlined. ES ≡ early stages.
[b] Good ≡ less than 1% removed; fair ≡ less than 50% removed; and poor ≡ more than 50% removed during replication.

Oxide Structure—EP Surfaces

In general the diffraction patterns show that the cubic spinel oxide, Fe_3O_4, was the sole or principal product of oxidation at temperatures up to and including 240°C (Tables I and II). Diffraction patterns of the oxide before and after oxidation at 240°C for both orientations are shown in Figs. 4a to 4d. The prior oxides, 16 Å thick, gave rise to diffuse, slightly arced, reflections and the subgrain size has been shown to be less than 30 Å.[4] The original epitaxy of the spinel oxide on both (001) and (112) Fe was retained on oxidizing at 200, 220, and 240°C and the epitaxial relationships are in agreement with those previously reported in the literature.[3,7,8] In

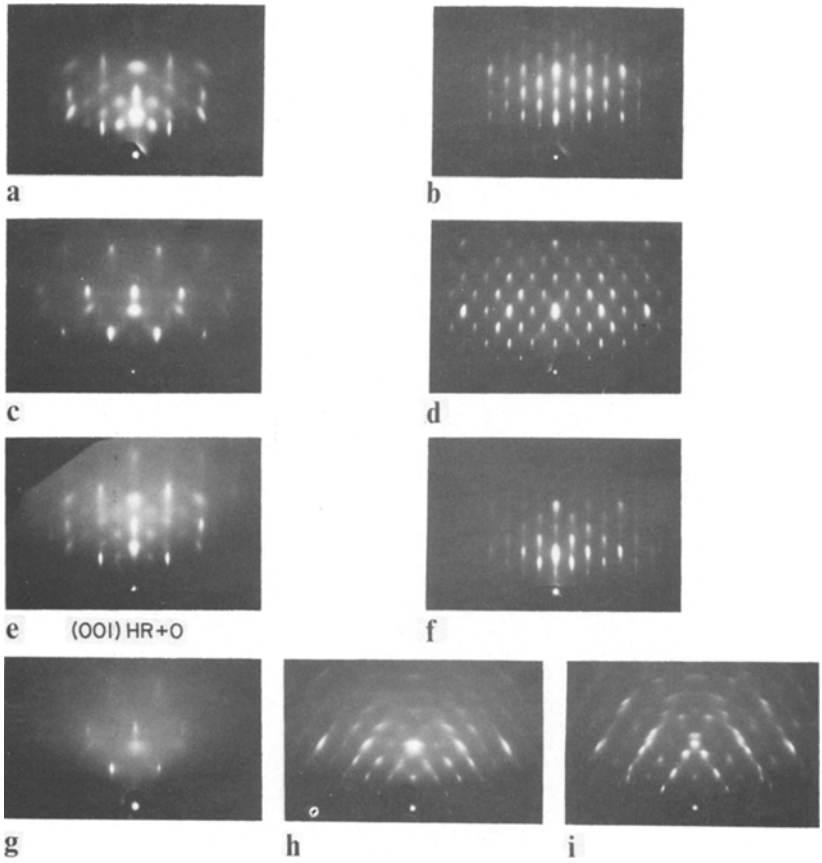

Fig. 4. Reflection electron diffraction patterns from (001) and (112) Fe surfaces after oxidation at 240°C. Electron beam along $[\bar{1}10]$ oxide zone. Oxide thicknesses and oxidation times are: (a) (001) EP; (b) (001) EP, 499 Å (2.13 hr); (c) (112) EP; (d) (112) EP, 420 Å (2.15 hr); (e) (001) HR+O; (f) (001) HR+O, 364 Å (2.05 hr); (g) (112) HR+O; (h) (112) HR+O, 265 Å (0.26 hr); (i) (112) HR+O, 401 Å (2.05 hr).

addition, the RED patterns for the EP (112) surfaces oxidized at 200 and 240°C showed diffuse streaks parallel to the ⟨111⟩ directions around certain spinel reflections centering on the (440) reflection (Fig. 4d). This streaking[3] is indicative of the early stages of formation of α-Fe_2O_3 (Table II). Single-orientation Fe_3O_4 was also produced after 2 hr oxidation at 260°C on both orientations and again early stage formation of α-Fe_2O_3 was evident on the (112) surfaces. At short times at 300°C only single crystal Fe_3O_4 was observed on both EP surfaces (Figs. 5a and 5b). After longer times single-

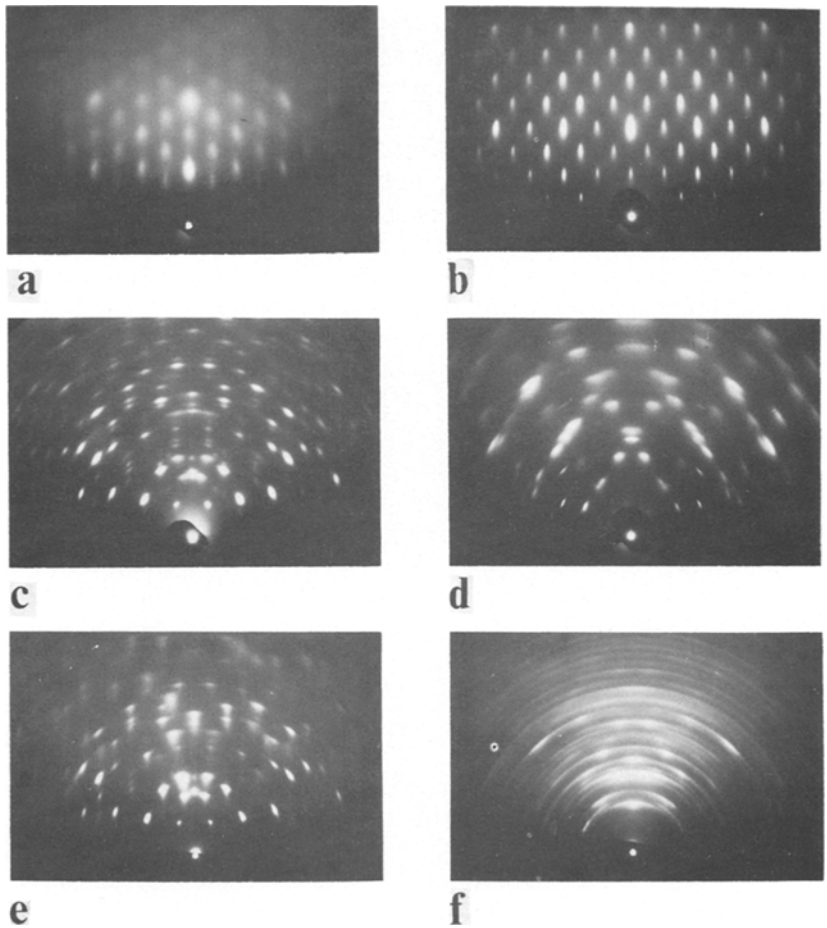

Fig. 5. Reflection electron diffraction patterns from (001) and (112) Fe surfaces after oxidation at 300°C. Electron beam along [$\bar{1}$10] oxide zone. Oxide thicknesses and oxidation times are: (a) (001) EP, 312 Å (0.11 hr); (b) (112) EP, 547 Å (0.17 hr); (c) (001) EP, 1996 Å (2.05 hr); (d) (112) EP, 2230 Å (1.41 hr); (e) (001) HR+O, 711 Å (2.00 hr); (f) (112) HR+O, 903 Å (2.10 hr).

crystal α-Fe_2O_3 had developed to such an extent that the pattern from the underlying Fe_3O_4 layer could not be detected (Figs. 5c and 5d). The above diffraction data are in agreement with the observations of Sewell and Cohen[3] and Ramasubramanian *et al.*[9], who show the development of α-Fe_2O_3 on (001) and (112) surfaces as the temperature is increased from 175 to 350°C. In most instances (Tables I and II) the oxide on EP surfaces appeared to be adherent. Replicas of the oxidized surfaces of both (001) and (112) Fe substrates are shown in Fig. 6. Nuclei of α-Fe_2O_3 appearing as lenticular-shaped islands, oriented in two directions at 90° to one another, were evident on the (001) surface after oxidation at 260°C (Fig. 6c). A portion of this oxide was stripped during replication (Table I); transmission electron diffraction (TED) did not, however, demonstrate the presence of α-Fe_2O_3 due probably to the low proportion of this phase in the total oxide scale. Also α-Fe_2O_3 was not detected by RED. It is evident that the α-Fe_2O_3 nuclei escaped detection using this technique, because they lay below the oxide macrosurface, namely the Fe_3O_4 matrix. Fe_2O_3 islands were not observed on the (001) surface after 0.12 hr oxidation at 300°C (Fig. 6e); after 2 hr at this temperature, however, the α-Fe_2O_3 was well developed and covered the whole of the sample surface (Fig. 6g). The lenticular islands have grown and expanded laterally in the two preferred directions to give a cross-hatched surface morphology. Enough α-Fe_2O_3 was now present to be detected by TED, although Fe_3O_4 was still the major constituent (Table 1, and footnote *c*).

The early stages of α-Fe_2O_3 formation, demonstrated by the diffuse streaking on the diffraction patterns from the (112) EP surfaces oxidized for 2 hr at 240 (Fig. 4d) and 260°C could not be attributed to any corresponding surface feature (Figs. 6b and 6d), as was the case for the (001) surfaces. After a longer time at 300°C, however, when α-Fe_2O_3 was the only phase observed by RED (Fig. 5d), ridged features were observed oriented at about 60° to one another (Fig. 6h).

Oxide Structure—HR + O Surfaces

RED patterns from the prior oxides produced on HR + O surfaces (Figs. 4e and 4g) again showed diffuse, slightly arced spots, similar to those observed for EP surfaces. At 240°C, RED showed that only Fe_3O_4 was formed on the (001) HR + O surfaces (Fig. 4f). After long-term oxidation at 300°C, however, α-Fe_2O_3 was the predominant phase (Fig. 5e). For the (112) HR + O surfaces α-Fe_2O_3 formation occurred at all temperatures. After 0.26 hr oxidation at 240°C (Fig. 4h) the diffuse streaking through certain spinel reflections centering on the (440) reflection was well developed, indicative of the formation of α-Fe_2O_3.[3] After 2 hr oxidation

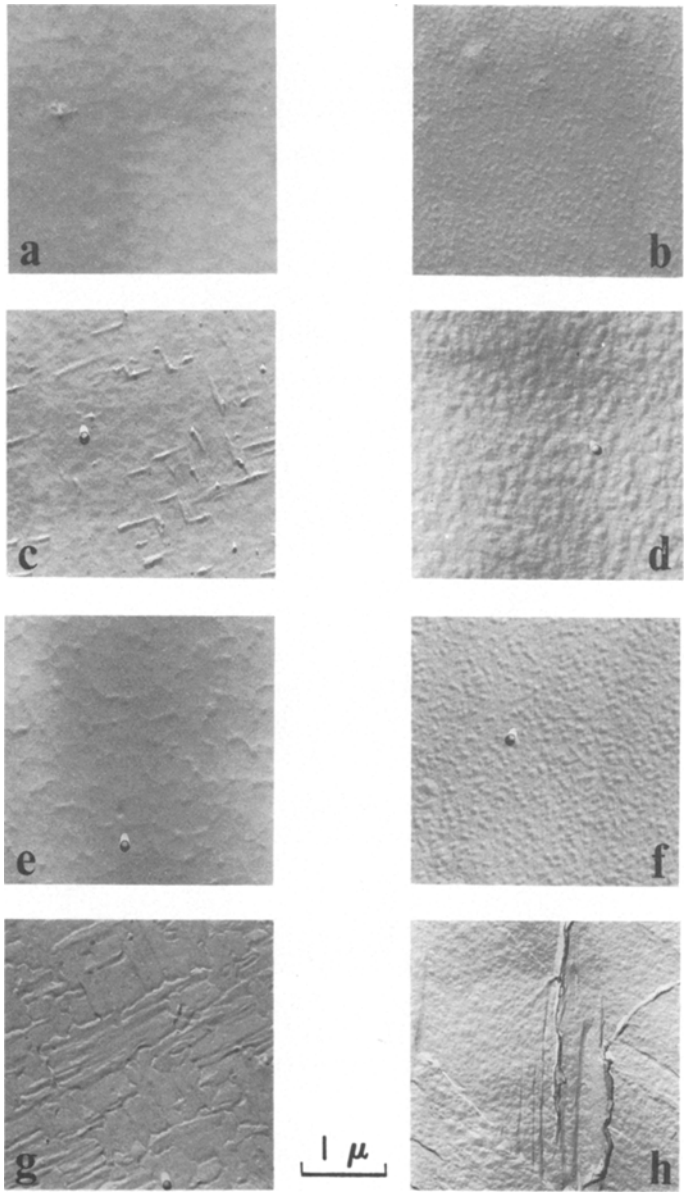

Fig. 6. replicas of the oxidized (001) and (112) EP Fe surfaces. a, c, e, and g are the (001) surfaces and b, d, f, and h are the (112) surfaces after oxidation at, respectively, 240, 260, 300°C (short term) and 300°C (long term).

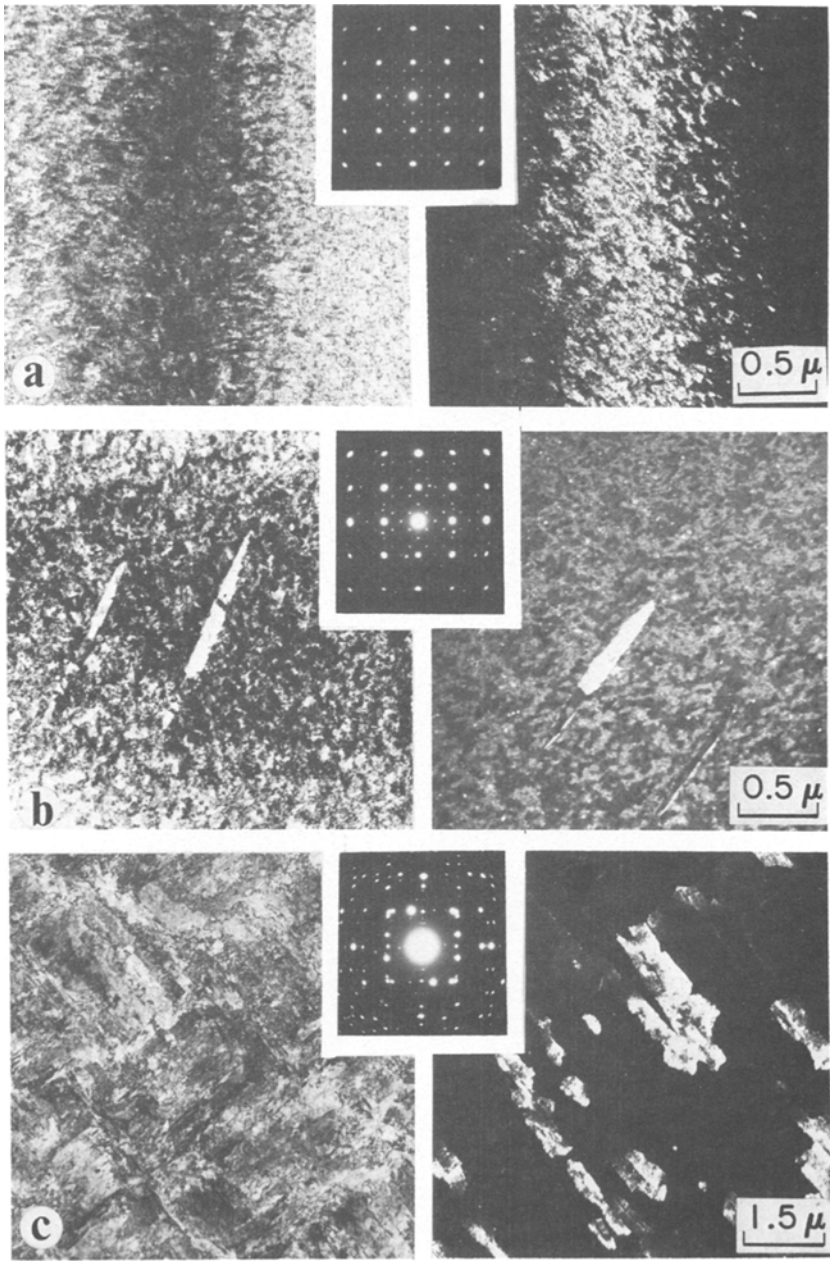

Fig. 7. Bright field micrographs (left-hand column) and dark field micrographs (right-hand column) with insets showing corresponding TED patterns of oxide films stripped from the (001) HR + O Fe surfaces after oxidation at (a) 240°C from (400) Fe_3O_4 reflection; (b) 260; and (c) 300°C from (104) α-Fe_2O_3 reflection.

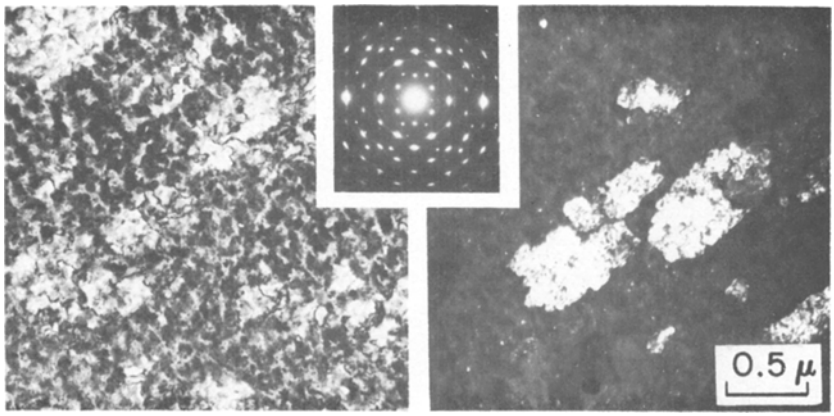

Fig. 8. Bright field micrograph (left-hand side) and dark field micrograph (right-hand side) from (012) α-Fe_2O_3 reflection with inset showing corresponding TED pattern of oxide film stripped from the (112) HR+O surface after oxidation at 260°C.

(Fig. 4i) the α-Fe_2O_3 pattern was predominant. Only α-FeO_3 was detected on the (112) HR+O surface at 300°C after 2 hr oxidation (Fig. 5f). Considerable arcing in the RED pattern was indicative of a fair degree of polycrystallinity in the α-Fe_2O_3. The above results are in good agreement with earlier work on the oxidation of Fe single crystals at 350°C.[9]

In every case, for either the (001) or (112) HR+O orientations oxidized for 2 hr, the oxide stripped easily and often completely from the metal substrate (Tables I and II). The oxide layer was only entirely adherent for the short term oxidation of the (112) surface at 240°C; in this case a replica of the oxide surface showed it to be similar to that for the (112) EP surface at the same temperature after 2 hr (Fig. 6b). Information about the structure of the stripped films was obtained by TED and by bright and dark field electron microscopy as shown in Figs. 7 and 8 for the (001) and (112) HR+O surfaces, respectively. The TED patterns for the oxide film from the (001) surface oxidized at both 240 and 260°C were similar except that an ordered array of extra reflections were observed in the latter case (cf. Figs. 7a and 7b). These reflections were identified as those from α-Fe_2O_3 and dark field micrographs showed that they arose from similarly oriented α-Fe_2O_3 islands in the Fe_3O_4. These islands were observed to be oriented at 90° to one another and their concentration in the oxide film was very small. A bright field micrograph of the oxide film produced at 300°C (Fig. 7c) showed the characteristic cross-hatched α-Fe_2O_3 structure to be similar to that observed for the oxidized (001) EP surface at 300°C (Fig. 6g). Single crystal patterns of both α-Fe_2O_3 and Fe_3O_4 could be distinguished, α-Fe_2O_3 being the major constituent in the oxide layer in contrast to that found in the oxide

layer produced on the EP surface. Dark field micrographs showed groups of similarly aligned crystallites (Fig. 7c). Oxide films formed on the (112) HR+O surfaces showed evidence of α-Fe_2O_3 formation at 240, 260, and 300°C. A characteristic α-Fe_2O_3 structure was not revealed in bright field micrographs, for example, at 260°C (Fig. 8), but reflections due to α-Fe_2O_3 were observed in addition to those of the Fe_3O_4 pattern. There was a degree of randomness in the patterns in contrast to those for the (001) HR+O surfaces. Dark field micrographs from the oxide produced at 260°C showed that the α-Fe_2O_3 was present as irregularly shaped areas. At 300°C α-Fe_2O_3 was the predominant phase, and the dark field micrographs suggest that it may have formed a continuous layer. Once again there was a fair degree of polycrystallinity in the oxide.

DISCUSSION

The oxidation kenetics for (001) EP Fe showed good agreement to a parabolic rate equation up to 2 hr oxidation at temperatures from 200 to 260°C. For (112) EP Fe the kinetic data showed only reasonable conformity to such an equation over similar times and temperatures. The parabolic behavior occurs in a region where Fe_3O_4 is the sole or principal oxide and where the oxidation rate is most likely controlled by cation diffusion through the Fe_3O_4. (The very small coverage of α-Fe_2O_3 nuclei (Fig. 6c), is not considered to have a serious effect on the kinetics). The dark field data indicates that the Fe_3O_4 layer consists of a mosaic of similarly oriented crystallites of grain size ranging from about 500 Å at 220°C [(112) surface] to about 1300 Å at 260°C [(001) surface]. At these low temperatures the low angle boundaries between the Fe_3O_4 crystallites are likely to be effective as preferred diffusion paths. Correlation of the rate constants for Fe_3O_4 growth on single-crystal Fe with those obtained on polycrystalline Fe surfaces will be given in the following paper.[10]

The decrease in oxidation rate to a low value at 300°C for both (001) and (112) EP Fe after about 0.8 hr (Fig. 3) can be correlated with the formation and lateral growth of the α-Fe_2O_3 islands. Previous work by Boggs *et al.*[11] on single-crystal Fe surfaces at 350°C and Graham and Cohen[12] on polycrystalline Fe at 350° and 400°C has suggested that the oxidation kinetics would be controlled by the density and growth rate of the α-Fe_2O_3 crystallites. At 300°C the coverage by the α-Fe_2O_3 appears to be complete at the end of the experiment, but the major proportion of the scale is still Fe_3O_4. The structure of the α-Fe_2O_3 "layer" on either orientation was similar to that observed by Boggs *et al.*[11], namely, the α-Fe_2O_3 was composed of a cross-hatched array of crystallites on the (001) surface (Fig. 6g) and an array of two sets of acicular crystallites aligned at about 60°

to one another on the (112) surface (Fig. 6h). The faceted surfaces of the α-Fe_2O_3 crystallites lie below the plane of the Fe_3O_4 matrix and they extend into it to a depth, which is dependent on the oxidation time. Other studies on polycrystalline Fe[10], in which the α-Fe_2O_3 was removed by cathodic reduction, demonstrated that after 1.8 hr at 300°C the α-Fe_2O_3 crystallites on certain orientations penetrated to the metal–oxide interface. These results and the present data show that the nucleation of α-Fe_2O_3 occurred at sites on suitably oriented facets of the Fe_3O_4 surface. Thus the α-Fe_2O_3 layer produced at long times will consequently be nonuniform in thickness. The establishment of a well-developed α-Fe_2O_3 layer at 300°C is probably assisted by some void nucleation at the metal–oxide interface.

In contrast to EP surfaces the oxidation kinetics of HR + O surfaces do not demonstrate parabolic behavior at any temperature for either orientation. The rapid decrease in oxidation rate observed for the latter surfaces at all temperatures can be attributed principally to a separation of the oxide from the metal. The oxide adhesion was nearly always found to be poor (Tables I and II). It is believed that the subgrain size of the prior oxide produced on HR + O surfaces is smaller than that produced on EP surfaces. This permits a higher cation flux across the oxide, i.e., a faster initial rate of oxidation, leading to vacancy condensation at the metal–oxide interface and subsequent separation. This separation again assists the establishement of the well-developed α-Fe_2O_3 layer, which forms at 300°C. Under the present experimental conditions formation of α-Fe_2O_3 on the (001) HR + O surfaces does not occur at all at 240°C, only to a very small extent at 260°C, and is well established at 300°C. For the (112) HR + O surface the proportion of α-Fe_2O_3 also increases with increasing temperature. Thus, for both EP and HR + O surfaces, the extent of α-Fe_2O_3 formation will depend upon the oxidation temperature, the oxygen pressure, [11,12] the oxide crystallite size, and the degree of oxide separation. Whether (001) or (112) Fe oxidizes faster for a given surface pretreatment will depend on which of these factors exerts the most influence on the oxidation kinetics.

It is interesting to compare the present results on the influence of oxide structure and surface pretreatment on the oxidation behavior of Fe with previous studies on Ni.[1] For (001) and (112) Fe and (112) and (111) Ni EP surfaces, under conditions where the oxide layers are single phase (respectively, Fe_3O_4 and NiO), oxide overgrowths of similar thickness are single-crystal and adherent. For HR + O pretreated surfaces, the initial oxidation rate is higher than for EP surfaces due to a finer-grained prior oxide. In the case of Ni the difference in rate was dramatic [a factor $\sim 10^4$ for the (112) surface] and was associated with propagation of a polycrystalline oxide on HR + O Ni surfaces. For Fe, while the initial rate of oxidation of HR + O surfaces is higher, the rapid rate is not sustained because of oxide separation from the metal and α-Fe_2O_3 formation at higher temperatures.

SUMMARY

A study of the oxidation behavior of the (001) and (112) Fe surfaces at 200 to 300°C in 5×10^{-3} Torr O_2 pressure has shown that the oxidation rate depends little on metal orientation, whether the prior oxide film was formed by electropolishing (EP surface pretreatment) or by dry oxidation in O_2 at room temperature (HR + O surface pretreatment). For both orientations, however, there was a strong dependence of the oxidation rate on the surface pretreatment, confirming that the nature of the prior oxide film is the prime factor determining subsequent oxidation behavior. It is believed that the faster initial rate for the HR + O surfaces is attributable to a smaller subgrain size and hence higher leakage path density in the prior oxide. This higher initial rate eventually leads to vacancy condensation and separation at the metal–oxide interface, which explains the rate decrease to a low value. With increasing temperature α-Fe_2O_3 formation becomes significant, its relative amount being greater for the HR + O surfaces and enhanced by the separation.

ACKNOWLEDGMENT

The authors wish to thank G. I. Sproule for the preparation of the replicas.

REFERENCES

1. M. J. Graham, R. J. Hussey, and M. Cohen, *J. Electrochem. Soc.* **120**, 1523 (1973).
2. P. B. Sewell and M. Cohen, *J. Electrochem. Soc.* **111**, 501 (1964).
3. P. B. Sewell and M. Cohen, *J. Electrochem. Soc.* **111**, 508 (1964).
4. P. B. Sewell, C. D. Stockbridge, and M. Cohen, *J. Electrochem., Soc.* **108**, 933 (1961).
5. P. B. Sewell, C. D. Stockbridge, and M. Cohen, *Can. J. Chem.* **37**, 1813 (1959).
6. M. J. Graham and M. Cohen, *J. Electrochem. Soc.* **119**, 879 (1972).
7. J. B. Wagner, Jr., K. R. Lawless, and A. T. Gwathmey, *Trans. Metall. Soc. AIME* **221**, 257 (1961).
8. M. J. Graham, S. I. Ali, and M. Cohen, *J. Electrochem. Soc.* **117**, 513 (1970).
9. N. Ramasubramanian, P. B. Sewell, and M. Cohen, *J. Electrochem. Soc.* **115**, 12 (1968).
10. R. J. Hussey, D. Caplan, and M. J. Graham, *Oxid. Met.* **15**, 421 (1981) (following paper in this issue).
11. W. E. Boggs, R. H. Kachik, and G. E. Pellissier, *J. Electrochem., Soc.* **114**, 32 (1967).
12. M. J. Graham and M. Cohen, *J. Electrochem. Soc.* **116**, 1430 (1969).